

Sema4C induces the endothelial-mesenchymal transition of tumor-associated lymphatic endothelial cells in cervical cancer via the ERK pathway

Jin Peng

Shandong University Qilu Hospital

Xijiang Liu

Shandong Provincial Hospital

Chengcheng Li

Shandong University Qilu Hospital

Min Gao

Shandong University Qilu Hospital

Hongyan Wang (✉ hongyanwang@sdu.edu.cn)

Shandong University Cheeloo College of Medicine <https://orcid.org/0000-0002-0923-0932>

Primary research

Keywords: Sema4C, primary tumor associated lymphatic endothelial cells, endothelial-mesenchymal transition, ERK

Posted Date: August 21st, 2020

DOI: <https://doi.org/10.21203/rs.3.rs-52892/v2>

License:  This work is licensed under a Creative Commons Attribution 4.0 International License.

[Read Full License](#)

1 **Sema4C induces the endothelial–mesenchymal transition of tumor-associated**
2 **lymphatic endothelial cells in cervical cancer via the ERK pathway**

3
4 Jin Peng^{1#} Xijiang Liu^{2#} Chengcheng Li¹ Min Gao¹ Hongyan Wang^{1*}

5
6 ¹ Department of Obstetrics and Gynecology, Qilu Hospital, Cheeloo College of
7 Medicine, Shandong University, Jinan, 250001, China

8 ² Department of Anesthesiology, Shandong Provincial Hospital affiliated to Shandong
9 First Medical University, Jinan 250021, China

10 #These authors contribute equally to this work.

11
12 *Corresponding Author

13 Hongyan Wang

14 Department of Obstetrics and Gynecology,
15 Qilu Hospital, Cheeloo College of Medicine,
16 Shandong University

17 No.107 West Wenhua Road, Jinan, 250001, China

18 Tel:+86-0531-88361855

19 Fax:+86-0531-86927544

20 E-mail: hongyanwang@sdu.edu.cn

21
22
23
24
25
26
27
28
29

30 **Abstract**

31 **Background:** The endothelial-mesenchymal transition (EndMT) is a process that
32 increases the promigratory abilities of endothelial cells (ECs). Although lymphatic
33 endothelial cells (LECs) plays a positive role in tumor lymphatic metastasis, the
34 regulation of LECs undergoing EndMT remains poorly understood. Previous study
35 indicated that Semaphorin 4C (Sema4C) could be a marker of LECs in cervical cancer.
36 Here, we try to understand the mechanism that Sema4C could promote LECs to get
37 mesenchymal characters and enhance lymphatic metastasis in cervical cancer.

38 **Methods:** The co-location of Sema4C and lymphatic marker LYVE1 was verified by
39 confocal laser scanning. Primary tumor-associated LECs (TLECs) were distinguished
40 from cervical cancer by flow cytometry from a mouse xenograft cervical tumor model.
41 The promigratory ability was assessed using the Transwell test. Lentivirus infection
42 was used to alter the expression of Sema4C in TLECs and the infection efficiency was
43 tested by confocal laser scanning. The phospho-extracellular signal-regulated kinase
44 (p-ERK) signaling pathway was measured using the ERK inhibitor (PD98059), as
45 well as quantitative PCR and Western blot analysis.

46 **Results:** Sema4C and LYVE1 co-located on TLECs. Primary TLECs were
47 successfully separated and cultured. Overexpressing Sema4C by lentivirus infection
48 stimulated the invasive capacity of TLECs and downregulated E-cadherin, whereas
49 knocking down Sema4C had the opposite effects. TLECs pro-migratory ability was
50 found to depend on the extracellular signal-regulated kinase (ERK) signaling pathway,
51 as the ERK inhibitor (PD98059) reversed Sema4C-induced E-cadherin expression and
52 migration ability.

53 **Conclusion:** The results of this study suggest that the Sema4C-ERK-E-cadherin
54 pathway appears to be critical for the EndMT of TLECs, which might promote lymph

55 node metastasis. Thus, Sema4C could be a promising target for the treatment of
56 cervical cancer with lymphatic metastasis.

57

58 **Keywords:** Sema4C, primary tumor associated lymphatic endothelial cells,
59 endothelial-mesenchymal transition, ERK.

60

61 **Background**

62 Lymphatic metastasis is one of the crucial routes of metastasis in cervical cancer
63 (1). Treatment failure in cervical cancer is often due to lymph node metastasis (2).
64 Lymphatic vessels are usually viewed as playing a passive role in metastasis, serving
65 merely as a channel for tissue-invading tumor cells (3). Recent studies have focused
66 on the immune-regulatory function of lymphatic endothelial cells (LECs), which are
67 active players in lymphatic metastasis(3, 4) . However, it remains unclear whether and
68 how LECs actively regulate lymphatic metastasis in cancer.

69 The endothelial – mesenchymal transition (EndMT) is a process by which
70 endothelial cells (ECs) display considerable plasticity in the transition to
71 mesenchymal cells; this was originally observed during heart development, whereas
72 recent studies have suggested its role in cancer and fibrosis. During this process, ECs
73 lose their endothelial markers such as E-cadherin and cluster of differentiation and
74 acquire a migratory phenotype, along with mesenchymal markers such as vimentin
75 and fibroblast special protein (5, 6). LECs also express E-cadherin and can be induced
76 to enter the epithelial – mesenchymal transition (EMT) by WNT5B and Kaposi’s
77 sarcoma-associated herpesvirus (7, 8). E-cadherin is a major component of epithelial
78 cell junctions, as well as a hallmark of the EndMT (6). However, our current
79 understanding of the regulatory mechanism underlying E-cadherin expression in
80 EndMT is still limited. In the EMT, which is analogous to EndMT, epidermal growth
81 factor is suggested to induce the downregulation of E-cadherin through the
82 extracellular signal-regulated kinase (ERK) pathway (9), which might activate a
83 similar signaling pathway in the EndMT.

84 Semaphorins (Semas) are a large family of extracellular signaling proteins that
85 regulate the motility of cells during the development of nevi (Sema3A, 3F, 6C, 6D),
86 the neuroendocrine system (Sema7A and Sema4D), the immune system (Sema4D),
87 reproductive systems (Sema3), and cancer progression (Sema4D, 3A, 6D) (10-12).

88 Interestingly, Semas antagonize the effect of vascular endothelial growth factor
89 (VEGF) (13). In addition, several recent studies have suggested that Sema3F may
90 affect lymphangiogenesis (14, 15). In previous study, TLECs were isolated and
91 normal LECs using *in situ* laser capture microdissection, and determined that
92 synthetic membrane-bound Sema4C functions as an autocrine factor that promotes
93 lymphangiogenesis (16). Nevertheless, the mechanism of Sema4C in regulating
94 TLECs biological characteristics is largely unknown.

95 It is well known that tumors or metastasis must rely, at least in part, on the gene
96 regulatory events in cells that constitute the primary tumor, as well as the tumor
97 microenvironment (TME) (17). LECs, which are one of the most important
98 components in the TME, also have special gene expression compared with non-tumor
99 LECs such as VEGFR3, which is activated under pathological situations including
100 cancer and inflammation (18). LECs in the market are separated from human lymph
101 nodes (Catalog #2500; ScienCell Research Laboratories, Carlsbad, CA, USA). The
102 differential expression of genes between normal LECs and TLECs prompted us to
103 assess the TLECs from tumors. Flow cytometry has been proven to be the best way
104 for isolating cells, as well as analyzing the TME (19). For the first time, primary TLEs
105 separated from mouse cervical tumor were used in this study for LEC biological
106 characterization.

107 This study evaluated the role of Sema4C in the transdifferentiation of primary
108 TLECs to determine mesenchymal characteristics. We reported that Sema4C
109 promotes TLECs invasiveness and regulates the ERK-E-cadherin pathway. We
110 propose that this pathway is involved in EndMT-like development. Our findings
111 indicate that the control of the Sema4C-ERK-E-cadherin pathway may be a novel
112 target for cancer therapy, which may potentially inhibit endothelial
113 transdifferentiation to mesenchyme-like cells, thereby blocking the lymphatic
114 metastasis of cancer. This preclinical study provides new insights into Sema4C in
115 TLECs and confirms the active participation of TLECs in lymphatic metastasis.

116

117 **Materials and Methods**

118 **Antibodies and cell line**

119 All reagents in this study are of analytical grade and commercially available. The
120 primary antibodies used in this study were as follows: Sema4C antibody (sc-

121 136445,Santa Cruz Biotech, USA); LYVE1 antibody for flow cytometry (53-0433-
122 82,ebioscience,USA, 5ul/5-8×10⁶ cells/ml); LYVE1 antibody for
123 immunohistochemistry (ab14917,abcam, USA). Vascular endothelial growth factor
124 receptor 3(VEGFR3, ab51874), E-cadherin(ab181296), ERK1/2(ab17942), p-
125 ERK1/2(ab214362) and b-actin(ab8227) antibodies were from abcam, USA. The
126 alkaline phosphatase-conjugated anti-rabbit(A9919), anti-mouse(A4312) were
127 purchased from Sigma, USA. ERK inhibitor, PD98059 (HY-12028), was purchased
128 from MCE, USA. Mouse cervical cancer cell line U14 was purchased from Yubo
129 company, Shanghai (YB-M060). The cells were cultured in RPMI 1640 medium
130 (Gibco-BRL, US) with 10% (v/v) fetal bovine serum (Gibco-BRL, US).

131 **Lentivirus for delivery of full-length Sema4C and siRNA against Sema4C**

132 Overexpression and silencing Sema4C lentivirus were purchased from Western
133 Biomedical technology, China. A full-length mouse Sema4C open reading frame was
134 obtained by PCR, using cDNA as templates, the primers sequences were : forward
135 (5'-
136 AGGGTTCCAAGCTTAAGCGGCCGCGCCACCATGGCCCCACACTGGGCTGT
137 CTGG-3')

138 reverse(5'-
139 GATCCATCCCTAGGTAGATGCATTCATACTGAAGACTCCTCTGGGTTG-3').
140 Lentivirus for delivery of full-length Sema4C was LV5. The final construction was
141 termed as LV5-Sema4C. The control construction was LV5NC. Lentivirus for
142 delivery of siRNA against Sema4C was LV3.The Sema4C siRNA was 5'-
143 CCTATGCCTTCCAGCCCAA-3', termed as LV3-Sema4C siRNA, and the sequence
144 for control siRNA (5'-TTCTCCGAACGTGTCACGT-3') named as LV3NC. The
145 Sema4C siRNA had been verified in previous article (9).

146 **Animals**

147 C57BL/6 female mice were purchased from Tengxin Biomedical technology,
148 Chongqing, China. The mice were maintained in the accredited animal facility of
149 Shandong University.The animal room had a controlled temperature (23-25°C),
150 photoperiod reversed 12/12 h light/dark cycle with lights on from 8:00 to 20:00; and
151 relative humidity (50–60%). The hygienic status was specific pathogen-free (SPF)

152 according to the Association for Assessment and Accreditation of Laboratory Animal
153 Care International (Laboratory Animal Facility of Tsinghua University)
154 recommendations. They were used at age 4-6 wk, 18-22 gram weight. All of the
155 experiments carried out in accordance with the International Council for Laboratory
156 Animal Science (ICLAS) considering the animal rights. All of the experimental
157 protocols were approved by Animal Care and Use Commit of Shandong University
158 for animal ethics.

159 **Mouse xenograft tumor model**

160 Animals were anesthetized using 2% isoflurane/O₂ flow in an induction chamber for
161 10min. Use the forceps to touch the leg of the mouse , confirm that the mouse is fully
162 unconscious. Mice received 100ul ($\approx 1 \times 10^7$) of U14 cells s.c. into the left shoulder.
163 After the tumors had grown to a palpable size below the skin surface ($\approx 15\text{mm}^3$, 4
164 weeks after injection), keep mice in their home cage for euthanasia, and put their cage
165 in a chamber with CO₂. Turn on the compressed CO₂ for at least 20 min and 2L/min.
166 The percentage of the chamber volume displaced by minute by flow rate of CO₂ was
167 20%. Let the CO₂ on until at least 1 min after mice stop breathing. Place the
168 sacrificed-mouse on a polystyrene board, cut the tumor and measure it.

169 **Separating TLECs by flow cytometry**

170 Tumor tissues connective was break down by 1% collagenase IV for 30min, and
171 0.25% pancreatic enzymes for 5-8min. Cell suspensions was filtration through cell
172 sieves, 200- μ m mesh. After incubation for 48h at 37°C in 5% CO₂ for 48h, the suspend
173 cells were removed. Cells were then incubated with the monoclonal antibody against
174 mouse LYVE1-PE, after adjusting cell density as $5-8 \times 10^6/\text{ml}$. The samples were
175 analyzed on a FACSC alibur apparatus (BD Biosciences) and cells that expressed
176 LYVE1 were separated. LECs were cultured in EBM-2 medium (LONZA,
177 Switzerland) at 37°C in 5% CO₂ with 2% (v/v) fetal bovine serum (Gibco-BRL, US).

178 **Immunohistochemistry for quantification of lymphatic microvessel density** 179 **(LMVD)**

180 An immunohistochemical analysis of LYVE1 was performed using the avidin-biotin-
181 peroxidase complex method. Dewaxed and rehydrated mouse tumor tissue sections

182 were incubated overnight at 4°C with a rabbit monoclonal anti-mouse LYVE1
183 antibody at a 1:100 dilution or with PBS for negative control, then washed with PBS.
184 Biotinylated anti-rabbit immunoglobulin (DAKO, Kyoto, Japan) was then added to
185 the sections for 30 minutes at room temperature. Peroxidase-conjugated avidin
186 (DAKO, Kyoto, Japan) was then applied after the sections were washed with PBS.
187 The peroxidase activity was detected by exposing the sections to a solution of 0.05%
188 3, 3-diaminobenzidine and 0.01% H₂O₂ in Tris-HCl buffer (3, 3-diaminobenzidine
189 solution) for 10 minutes at room temperature. The sections were counterstained with
190 hematoxylin.

191 The stained sections were then analyzed using standard light microscopy (Nikon,
192 Eclipse 200). Under low magnification, the most vascularized intratumoral areas were
193 chosen (hot spots). The number of immunostained lymphatic vessels found in 3 hot
194 spot areas at 400× magnification were counted. The LMVD for each case was
195 expressed by the mean value (total number of vessels in 3 hot spot microscopic
196 fields/3).

197 **Confocal microscopy imaging**

198 For immunofluorescence staining, frozen tissue sections were used. The first
199 antibody was applied to the slides at 4°C overnight (LYVE1: 1:50, Sema4C: 1:20).
200 After the incubation with the first antibody, the cells were washed three times with
201 cold PBS and incubated with FITC- or Cy3-conjugated IgG at a 1:50 dilution in PBS
202 for 30 min at room temperature. The nuclei were stained for 5 min at room
203 temperature with DAPI. The cells were rinsed with PBS and observed using a
204 confocal microscope (Olympus, Japan).

205 **Immunohistochemistry for identification of TLECs**

206 An immunohistochemical identification analysis of LECs was performed using the
207 avidin-biotin-peroxidase complex method. LECs were incubated on sheet glasses in
208 12-well plate and fixed by 4%paraformaldehyde for 20 min at room temperature. The
209 cells were then incubated overnight at 4°C with polyclonal anti-mouse VEGFR3
210 antibody at a 1:30 dilution and then washed with PBS. HRP-immunoglobulin (abcam,
211 USA) was then added to the sections for 30 minutes at 37°C. After the sections were
212 washed with PBS, peroxidase-conjugated avidin (DAKO) was then applied. The

213 peroxidase activity was detected by exposing the sections to a solution of 0.05% 3, 3-
214 diaminobenzidine and 0.01% H₂O₂ in Tris-HCl buffer (3, 3-diaminobenzidine
215 solution) for 10 minutes at room temperature. The sections were counterstained with
216 hematoxylin.

217 **Cell transfection**

218 The primary TLECs were cultured in 24-well tissue culture plates or flasks at 37°C
219 with 5% CO₂ in a humidified incubator (Heraeus, Germany). For the lentivirus
220 infection, the cells (10⁵/ml/200ul) were added with lentivirus at MOI=40, when the
221 cells were 70% confluent according to the preliminary experiment. The cells were
222 infected for 72hrs for the next experiments. The control of lentivirus for delivery full-
223 length LV5-Sema4C is LV5control (LV5NC), while the control of LV3-siRNA
224 Sema4C is LV3control (LV3NC). The package system is four plasmid system, LV5-
225 GFP/LV3-GFP, PG-p1-VSVG, PG-REV, PG-P3-RRE. The results of transfection
226 were detected using a confocal microscope (Olympus, Japan).

227 **Quantitative Real-time PCR**

228 For quantitative real-time PCR, total RNA was isolated from cell lines in Trizol
229 reagent (Invitrogen, CergyPontoise, France). First-strand cDNA synthesis was
230 performed using a cDNA synthesis kit (Amersham Bioscience, NJ). Quantitative real-
231 time PCR was performed on an ABI PRISM 7700 Sequence Detection System
232 (Applied Biosystems, CA) by using a QuantiTect SYBR Green kit (Qiagen, CA). The
233 primers were designed using Primer Express 3.0 software, identified by Basic Local
234 Alignment Search Tool (BLAST) (<http://www.ncbi.nlm.nih.gov/BLAST>) and pur-
235 chased from Invitrogen. Each sample was run in triplicate. Conditions for quantitative
236 PCR reaction were as follows, one cycle of 50°C for 15 min, one cycle of 94°C for 4
237 min, 35 cycles of 94°C for 20 s, 60°C for 30 s, and 70°C for 35 s. At the end of the
238 PCR reaction, samples were subjected to a melting analysis to confirm specificity of
239 the amplification. The Sema4C primer sequences were: Forward:
240 CCTCCCATCTGTATGTCTGCG ; Reverse: GCTGGGTCATATGGGCATTTAC .
241 For internal standard, the actin primer sequences were: Forward:
242 GAGACCTTCAACACCCAGC; Reverse: ATGTCACGCACGATTTCCC.

243 **Immunoblotting**

244 For the Western blot analyses, the cells were lysed in RIPA buffer (50 mM Tris/HCl,
245 pH 7.2, 150 mM NaCl, 1% NP-40, 0.1% SDS, and 0.5% (w/v) sodium deoxycholate).
246 Equivalent amounts of the cell extracts (150 mg) were separated on a 10% sodium
247 dodecyl sulfate polyacrylamide gel (SDS-PAGE) and transferred onto a
248 polyvinylidenedifluoride membrane (PVDF). The membranes were blocked in 25 mM
249 Tris (pH 8.0) containing 125 mM NaCl, 0.1% Tween 20, and 5% skim milk for 1 hour
250 and then incubated with the diluted primary antibodies (Sema4C: 1:500, E-cadherin,
251 ERK1/2 and p-ERK1/2: 1:2000 and β -actin: 1:1000) at 4°C overnight. After
252 incubation with the primary antibodies, the secondary antibodies were added at a
253 1:1000 dilution. The immune reactive bands were visualized with Enhanced
254 chemiluminescence (ECL) western-blot technique.

255 **The migration assay**

256 For the migration assay, 5×10^3 cells were seeded in 100 ml EBM-2 media on the top
257 of polyethylene terephthalate (PET) membranes within transwell cell culture inserts
258 (24-well inserts, 8 mm pore size; Corning Life Sciences, Corning, NY). The bottom
259 chamber was filled with 600 ml EBM-2 media containing 2% FBS and the
260 supernatant from NIH3T3 cells (mouse embryonic fibroblast cell line) to act as a
261 chemotactic factor (CF). The cells were incubated for 48hrs at 37°C with 5% CO₂.
262 Subsequently, the cells were fixed in 2.5% (v/v) glutaraldehyde and stained with
263 crystal violet. Cells on the gel bottom were visualized under a microscope (Leica,
264 Germany) and quantified by counting the number of cells in three randomly chosen
265 fields at a 100-fold magnification.

266 **Statistical analysis**

267 Data were expressed as mean \pm SEM and statistical analysis was performed using
268 SPSS version 13.0 software. Statistical comparisons include one-way ANOVA
269 followed by post hoc comparison (Dunnett test and LSD-test).

270 **Results**

271 **Separation of TLECs from a mouse xenograft cervical tumor model**

272 Firstly, we determined the expression of Sema4C on TLECs in this mouse cervical
273 tumor tissue. Using a confocal microscope, LYVE1 was used to detected lymphatic
274 vessels, and co-location (merge) was found between Sema4C (green) and LYVE1

275 (red) (Fig. 1A). We employed primary TLECs to maintain the entire TME of cervical
276 tumors, including the immune and growth conditions, as well as interactions among
277 cells using BALB/C mice with U14 tumor allografts. The U14 cells were injected
278 subcutaneously (s.c.) into the left shoulder and lymphatic microvessel density was
279 tested by LYVE1 immunohistochemistry for the most appropriate time point to
280 separate TLECs (Fig. 1B). By LMVD analysis (Fig.1C), after tumor growing to the
281 7th day, the lymphatic vessels became intensively. After 14 days, massive necrosis
282 happened and the density of lymphatic vessels was decreased significantly. Then the
283 appropriate time for separation of TLECs was the 7th day after tumor cells injection.
284 LYVE1-positive cells were separated by flow cytometry (Fig. 1D). The cells were
285 cultured successfully, appeared as a typical monolayer (Fig.1E). VEGFR3 was
286 further used to identify the separated cells (Fig. 1F), and most of the cells were
287 positive for VEGFR3. Thus, the separated cells were both LYVE1 and VEGFR3
288 positive cells.

289

290 **Sema4C regulates the migration ability of TLECs**

291 We regulated the expression of the target gene Sema4C via lentivirus infection, non-
292 infected cells was used as blank controls (Fig. 2A). Small interfering RNA (siRNA)
293 Sema4C lentivirus (LV3-siRNA) and full-length Sema4C lentivirus (LV5-Sema4C),
294 as well as control lentivirus (LV3NC and LV5NC), all expressed green fluorescent
295 protein (GFP) at a multiplicity of infection of 40MOI for 72 h. The efficiency of the
296 silencing lentivirus and the overexpression lentivirus infection was 90% according to
297 the fluorescence test. Quantitative PCR (qPCR) showed almost 0.3- and 3.5-fold
298 higher RNA levels in LV3-siRNA and LV5-Sema4C relative to the control,
299 respectively (Fig. 2B). We then studied the effects of Sema4C on the invasiveness of
300 the TLECs using a classic Transwell model. The quantity of cells at the bottom of the
301 membrane, which reflects the migration of cells, was 56 ± 8.61 , 52 ± 7.38 , 51.2 ± 5.89 ,
302 40 ± 8.16 , and 73 ± 12.78 for con, LV3NC-siRNA-, LV5NC-siRNA-, LV3-siRNA-,
303 and LV5-Sema4C-treated cells, respectively (Fig. 2C). Silencing Sema4C inhibited
304 the migratory ability of TLECs and induced the overexpression Sema4C.

305

306 **Sema4C regulates EndMT of TLECs**

307 The migratory ability of ECs facilitates cellular movement similar to mesenchymal
308 cells (i.e., EndMT). Based on the previously mentioned literature, a possible

309 signalling pathway in the EndMT was investigated . Sema4C inhibited the expression
310 of E-cadherin, whereas silencing of Sema4C promoted expression. Moreover, the
311 level of phosphorylated ERK (p-ERK1/2), the active form of ERK1/2, was altered
312 with lentivirus infection of Sema4C full-length gene or Sema4C siRNA. Sema4C
313 stimulated the phosphorylation of ERK. A similar pattern was observed for mRNA
314 and protein levels using qPCR (Fig. 3A) and western blotting (Fig. 3B and 3C),
315 respectively.

316

317 **The ERK inhibitor reverses the Sema4C-induced EndMT**

318 We hypothesized that Sema4C regulates the EndMT partially through the regulation
319 of E-cadherin, which is one of the most important characteristics of EndMT. The
320 ERK inhibitor, PD98059 (30 mM), was employed to determine the alterations in
321 migration ability after Sema4C silencing or overexpression by lentivirus infection.
322 The results showed that PD98059 effectively enhanced the inhibition of migration
323 ability of Sema4C siRNA infection comparing to control group (Fig.4A). Furthermore,
324 the addition of PD98059 partially relieved the induced migration ability of TLECs
325 after overexpression of Sema4C (Fig. 4A). The quantities of cells at the bottom of the
326 membrane, as shown in the bar on the right side, reflected the migration of the cells,
327 which were 56 ± 8.61 , 40 ± 8.16 , 73 ± 12.78 , 18 ± 4.56 , and 58 ± 8.87 , for con, LV3-
328 siRNA-, LV5-Sema4C-, LV3-siRNA+PD98059-, and LV5-Sema4C+PD98059-
329 treated cells, respectively (Fig. 4B).

330

331 **The ERK inhibitor stimulates E-cadherin expression by blocking Sema4C**

332 The ERK inhibitor was used to determine whether Sema4C-mediated regulation of E-
333 cadherin depends on the phosphorylation level of ERK1/2. While silencing Sema4C
334 inhibited the phosphorylation level of ERK, the introduction of PD98059 further
335 enhanced the upregulation of E-cadherin expression by Sema4C siRNA infection.
336 However, inhibition of phosphorylation of ERK1/2 partially neutralized the
337 downregulation of E-cadherin that was regulated by Sema4C. The RNA levels of
338 Sema4C and E-cadherin were in accordance with the protein levels (Fig. 5A, 5B, 5E,
339 and 5F). Because the phosphorylation of ERK1/2 is a special characteristic of ERK1/2
340 at the protein level, we also tested the RNA levels of ERK1/2 (Fig. 5C). Recovery of
341 p-ERK1/2 expression in LV5-Sema4C plus PD98059 was observed compared to
342 LV5-Sema4C alone, indicating that PD98059 can effectively block Sema4C (Fig. 5D

343 and 5G). ERK1/2 RNA expression has increased after Sema4C overexpression, but
344 ERK1/2 protein level did not change significantly (Fig. 5H and 5I). However, it is
345 interesting that protein level of phosphorylation ERK1/2 show the same tendency as
346 ERK1/2 RNA level. Thus, phosphorylation level of ERK1/2 is more important in
347 Sema4C signaling pathway, rather than ERK1/2.

348

349 **Discussion**

350 Tumor-associated lymphangiogenesis is a key modulator of tumor metastasis,
351 although the underlying mechanism remains unclear. It was recently shown that the
352 lymphatic system actively participates in tumor metastasis(20), and that LECs play
353 important roles in inducing immune tolerance(21). The ability of LECs to promote
354 immunosuppression may induce tumor cell metastasis (22). A previous study using *in*
355 *situ* laser capture microdissection showed that the gene expression profile of human
356 tumor LECs differed from that of normal LECs, which was associated with increased
357 tube formation ability, and found that Sema4C was differentially expressed (19). Here,
358 we have focused on LECs undergoing EndMT to attain invasion ability, which was, at
359 least in part, due to the higher expression of Sema4C in tumor LECs.

360 EndMT was initially discovered as an essential step in heart development. Further
361 studies have demonstrated that EndMT occurs in cancer and tissue fibrosis (23), while
362 the regulation of this process requires further studies. Furthermore, as one of the most
363 important components of endothelial cells, whether and how LECs participate in the
364 EndMT during cancer development remains unclear. The biological characteristics of
365 LECs markedly change in tumors *in vivo* (17). Thus, in this study, we separated
366 TLECs from mouse cervical tumor tissues by flow cytometry, instead of an LEC cell
367 line from ScienCell, which was separated from normal lymphatic nodes. LYVE1 was
368 used as the marker for LEC separation (19) and VEGFR3 as an identification marker
369 (24).

370 It has been reported that some molecules show differences in molecular
371 mechanism between their membrane and soluble forms. For example, full-length
372 Sema3C is a tumor angiogenesis inhibitor, whereas cleaved Sema3C is a tumor
373 progression promoter (25). The previous study showed that there were biological
374 properties between the soluble and membrane forms of Sema4C (sSema4C and
375 mSema4C). sSema4C promotes lymphangiogenesis, whereas mSema4C also directs
376 cell-cell contacts, thereby providing the possibility of a new mechanism of mSema4C

377 working on LECs (15). Thus, we used lentiviral transfection for consistent
378 overexpression or silencing of mSema4C in TLECs.

379 In the previous study, Ras homolog family member A (RhoA) was critical to
380 Sema4C-mediated signaling. One of distinct cell migration models, named amoeboid-
381 type migration, is characterized by a spherical or elongated cell shape and is strongly
382 dependent on Rho kinase activity (26). Thus, we presume that LECs migrate and
383 undergo EndMT in the amoeboid-type, which could be promoted by Sema4C, as
384 shown by the Transwell test. A spherical cell shape with a small number of short
385 protrusions was found after passing through the polyethylene terephthalate
386 membranes. Mechanistically, we found that the promotion of the migration ability of
387 Sema4C-overexpressing LECs is in part attributable to ERK activation-induced
388 repression of E-cadherin expression.

389 E-cadherin is a cell adhesive molecule that plays a key role in cellular adhesion
390 and migration, which acts as one of the most important symbols of EndMT and can
391 also be regulated by RhoA(27). A recent study showed a novel role for E-cadherin in
392 regulating LEC progeny in newly synthesized lymphatic vessels (25, 28). In particular,
393 forced disruption of E-cadherin-mediated intercellular adhesion opened the
394 intercellular junctions in LEC monolayers as determined by another study using
395 Transwell assays (29). Here, we showed that repression of E-cadherin is a necessary
396 molecular event for the promotion of migration ability in Sema4C-overexpressing
397 LECs. This finding is concordant with another study, which demonstrated that the
398 overexpression of Sema4C suppresses E-cadherin, induces vimentin, and promotes
399 fibronectin secretion in human kidney cells (30). Although our results indicate that E-
400 cadherin is an important molecular target of Sema4C EndMT function, the
401 downstream signaling pathway was impacted by the loss of E-cadherin expression, as
402 well as promoted migrated ability, although the overexpression of Sema4C has yet to
403 be determined. The expression of E-cadherin is an ERK-dependent mechanism.
404 Hence, it will be interesting to determine whether the regulation of Sema4C-induced
405 E-cadherin expression and migration ability in LECs are activated by ERK. The
406 application of an ERK inhibitor has proven that Sema4C regulates E-cadherin, but
407 this process is dependent on ERK activation.

408

409 **Conclusions**

410 In summary, we confirm that Sema4C expressed on TLECs by co-location with
411 LVYE1, and provide evidence that overexpression of Sema 4C is an important
412 molecular mechanism that contributes to the EndMT of TLECs by suppressing E-
413 cadherin expression. Mechanistically, the process involves the activation of the ERK
414 pathway, which functions upstream of E-cadherin and downstream of Sema4C.
415 Studies on TLECs are limited, and thus, it will be important to determine whether
416 enhanced ERK activation during the upregulation of Sema4C as observed in TLECs
417 can induce tumor lymphatic metastasis, which in turn, can be targeted using
418 pharmacological approaches.

419

420 **List of abbreviations**

421 **Sema4C:** Semaphorin 4C

422 **EndMT:** endothelial-mesenchymal transition

423 **LECs:** lymphatic endothelial cells

424 **ECs:** endothelial cells

425 **TLECs:** tumor-associated Lymphatic endothelial cells

426 **ERK:** extracellular signal-regulated kinase

427 **EMT:** epithelial–mesenchymal transition

428 **Semas:** semaphorins

429 **VEGFR3:** vascular endothelial growth factor receptor 3

430 **VEGF:** vascular endothelial growth factor

431 **TME:** tumor microenvironment

432 **SPF:** specific pathogen-free

433 **LMVD:** lymphatic microvessel density

434 **SDS-PAGE:** sodium dodecyl sulfate polyacrylamide gel

435 **PVDF:** polyvinylidenedifluoride membrane

436 **ECL**: Enhanced chemiluminescence

437 **PET**: polyethylene terephthalate

438 **CF**: chemotactic factor

439 **qPCR**: Quantitative PCR

440 **p-ERK1/2**: phosphorylated ERK

441 **RhoA**: Ras homolog family member A

442 **siRNA**: small interfering RNA

443 **GFP**: green fluorescent protein

444

445 **Declarations**

446

447 **Ethics approval and consent to participate**

448 All of the experimental carried out in accordance with the International Council for
449 Laboratory Animal Science (ICLAS) considering the animal rights. All of the
450 experimental protocols were approved by Animal Care and Use Committe of
451 Shandong University for animal ethics.

452 **Consent for publication**

453 Not applicable

454

455 **Availability of data and materials**

456 The datasets used and/or analysed during the current study are available.

457

458 **Competing interests**

459 The authors declare that they have no competing interests

460

461 **Funding**

462 This work was supported by grants from the National Natural Science Foundation of
463 China (Nos. 81502238 and 81602286), and the Department of Medical and Health
464 Science Technology of Shandong province (No. 2016w0345), and from the

465 Department of Science Technology of Jinan city (No. 201705051) and from the China
466 Postdoctoral Science Foundation (No. 2019T120594).

467

468 **Authors' contributions**

469 HW designed the experiments and wrote the paper. JP and XL carried out the
470 molecular experiments and analyzed the data and conceived the experiments; CL built
471 the mouse model, performed the histological examination of tumor, and separated the
472 cells; MG provided soft ware analysis. All authors read and approved the final
473 manuscript.

474

475 **Acknowledgements**

476 We would like show sincere appreciation to Qingliang Wang for the statistic
477 assistance on this study.

478

479 **Authors' information**

480 Jin Peng and Xijiang Liu contributed equally to this work.

481 **References**

- 482 1. Frumovitz M. Sentinel Lymph Node Biopsy for Cervical Cancer Patients -
483 What's It Gonna Take? *Gynecol Oncol.* 2017 Jan;144(1):3-4.
- 484 2. Li H, Wu X, Cheng X. Advances in diagnosis and treatment of metastatic
485 cervical cancer. *J Gynecol Oncol.* 2016 Jul;27(4):e43.
- 486 3. Hoshino A, Lyden D. Metastasis: Lymphatic detours for cancer. *Nature.* 2017
487 Jun 28;546(7660):609-10.
- 488 4. Lucas ED, Tamburini BAJ. Lymph Node Lymphatic Endothelial Cell
489 Expansion and Contraction and the Programming of the Immune Response. *Front*
490 *Immunol.* 2019;10:36.
- 491 5. Saito A. EMT and EndMT: regulated in similar ways? *J Biochem.* 2013
492 Jun;153(6):493-5.
- 493 6. Kourtidis A, Lu R, Pence LJ, Anastasiadis PZ. A central role for cadherin
494 signaling in cancer. *Exp Cell Res.* 2017 Sep 1;358(1):78-85.
- 495 7. Wang SH, Chang JS, Hsiao JR, Yen YC, Jiang SS, Liu SH, et al. Tumour cell-
496 derived WNT5B modulates in vitro lymphangiogenesis via induction of partial
497 endothelial-mesenchymal transition of lymphatic endothelial cells. *Oncogene.* 2017
498 Mar;36(11):1503-15.
- 499 8. Lee HR, Li F, Choi UY, Yu HR, Aldrovandi GM, Feng P, et al. Deregulation
500 of HDAC5 by Viral Interferon Regulatory Factor 3 Plays an Essential Role in
501 Kaposi's Sarcoma-Associated Herpesvirus-Induced Lymphangiogenesis. *mBio.* 2018
502 Jan 16;9(1).
- 503 9. Wu H, Wang X, Liu S, Wu Y, Zhao T, Chen X, et al. Sema4C participates in
504 myogenic differentiation in vivo and in vitro through the p38 MAPK pathway. *Eur J*
505 *Cell Biol.* 2007 Jun;86(6):331-44.
- 506 10. Elder AM, Tamburini BAJ, Crump LS, Black SA, Wessells VM, Schedin PJ,
507 et al. Semaphorin 7A Promotes Macrophage-Mediated Lymphatic Remodeling during
508 Postpartum Mammary Gland Involution and in Breast Cancer. *Cancer Res.* 2018 Nov
509 15;78(22):6473-85.
- 510 11. Acker DWM, Wong I, Kang M, Paradis S. Semaphorin 4D promotes
511 inhibitory synapse formation and suppresses seizures in vivo. *Epilepsia.* 2018
512 Jun;59(6):1257-68.

- 513 12. Ferreira GD, Capp E, Jauckus J, Strowitzki T, Germeyer A. Expression of
514 semaphorin class 3 is higher in the proliferative phase on the human endometrium.
515 Arch Gynecol Obstet. 2018 May;297(5):1175-9.
- 516 13. Sakurai A, Doci CL, Gutkind JS. Semaphorin signaling in angiogenesis,
517 lymphangiogenesis and cancer. Cell Res. 2012 Jan;22(1):23-32.
- 518 14. Nasarre P, Gemmill RM, Drabkin HA. The emerging role of class-3
519 semaphorins and their neuropilin receptors in oncology. Onco Targets Ther.
520 2014;7:1663-87.
- 521 15. Doci CL, Mikelis CM, Lionakis MS, Molinolo AA, Gutkind JS. Genetic
522 Identification of SEMA3F as an Antilymphangiogenic Metastasis Suppressor Gene in
523 Head and Neck Squamous Carcinoma. Cancer Res. 2015 Jul 15;75(14):2937-48.
- 524 16. Wei JC, Yang J, Liu D, Wu MF, Qiao L, Wang JN, et al. Tumor-associated
525 Lymphatic Endothelial Cells Promote Lymphatic Metastasis By Highly Expressing
526 and Secreting SEMA4C. Clin Cancer Res. 2017 Jan 1;23(1):214-24.
- 527 17. Albini A, Mirisola V, Pfeffer U. Metastasis signatures: genes regulating
528 tumor-microenvironment interactions predict metastatic behavior. Cancer Metastasis
529 Rev. 2008 Mar;27(1):75-83.
- 530 18. Olmeda D, Cerezo-Wallis D, Riveiro-Falkenbach E, Pennacchi PC, Contreras-
531 Alcalde M, Ibarz N, et al. Whole-body imaging of lymphovascular niches identifies
532 pre-metastatic roles of midkine. Nature. 2017 Jun 28;546(7660):676-80.
- 533 19. Young YK, Bolt AM, Ahn R, Mann KK. Analyzing the Tumor
534 Microenvironment by Flow Cytometry. Methods Mol Biol. 2016;1458:95-110.
- 535 20. Lukacs-Kornek V. The Role of Lymphatic Endothelial Cells in Liver Injury
536 and Tumor Development. Front Immunol. 2016;7:548.
- 537 21. Humbert M, Hugues S, Dubrot J. Shaping of Peripheral T Cell Responses by
538 Lymphatic Endothelial Cells. Front Immunol. 2016;7:684.
- 539 22. Ji RC. Lymph Nodes and Cancer Metastasis: New Perspectives on the Role of
540 Intranodal Lymphatic Sinuses. Int J Mol Sci. 2016 Dec 28;18(1).
- 541 23. Cho JG, Lee A, Chang W, Lee MS, Kim J. Endothelial to Mesenchymal
542 Transition Represents a Key Link in the Interaction between Inflammation and
543 Endothelial Dysfunction. Front Immunol. 2018;9:294.
- 544 24. Harris AR, Perez MJ, Munson JM. Docetaxel facilitates lymphatic-tumor
545 crosstalk to promote lymphangiogenesis and cancer progression. BMC Cancer. 2018
546 Jul 6;18(1):718.

- 547 25. Mumblat Y, Kessler O, Ilan N, Neufeld G. Full-Length Semaphorin-3C Is an
548 Inhibitor of Tumor Lymphangiogenesis and Metastasis. *Cancer Res.* 2015 Jun
549 1;75(11):2177-86.
- 550 26. Lawson CD, Ridley AJ. Rho GTPase signaling complexes in cell migration
551 and invasion. *J Cell Biol.* 2018 Feb 5;217(2):447-57.
- 552 27. Lee G, Kim HJ, Kim HM. RhoA-JNK Regulates the E-Cadherin Junctions of
553 Human Gingival Epithelial Cells. *J Dent Res.* 2016 Mar;95(3):284-91.
- 554 28. Connor AL, Kelley PM, Tempero RM. Lymphatic endothelial lineage
555 assemblage during corneal lymphangiogenesis. *Lab Invest.* 2016 Mar;96(3):270-82.
- 556 29. Hou WH, Liu IH, Tsai CC, Johnson FE, Huang SS, Huang JS. CRSBP-
557 1/LYVE-1 ligands disrupt lymphatic intercellular adhesion by inducing tyrosine
558 phosphorylation and internalization of VE-cadherin. *J Cell Sci.* 2011 Apr 15;124(Pt
559 8):1231-44.
- 560 30. Zhou QD, Ning Y, Zeng R, Chen L, Kou P, Xu CO, et al. Erbin interacts with
561 Sema4C and inhibits Sema4C-induced epithelial-mesenchymal transition in HK2 cells.
562 *J Huazhong Univ Sci Technolog Med Sci.* 2013 Oct;33(5):672-9.

563

564

565 **Figure Legends**

566 **Fig.1 Tumor-associated lymphatic endothelial cells (TLECs) were obtained from**
567 **a mouse xenograft tumor.** (A) The location of Sema4C was detected in mouse tumor
568 tissue. In lymphatic vessels, Sema4C(green) have co-location with LYVE1(Red), one
569 of the most notable marker for lymphatic endothelial cells. Nuclei were shown by
570 DAPI staining (blue). (B)The most suitable time (the 7th day after U14 cells injection)
571 for separation of TLECs was determined by LYVE1 immunohistochemical analysis.
572 (C) Quantification of the numbers of lymphatic vessels (LMVD) in 5th, 7th, 14th days
573 were measured. (D)Tumor tissues were dissociated into a cell suspension and then
574 stained for LYVE1-PE. LYVE1-positive cells were separated by flow cytometry. (E)
575 TLECs were cultured in EBM-2 medium for 5 days and 10 days. (F) VEGFR3-
576 positive TLECs were identified by immunohistochemistry.

577 **Fig. 2 Role of Sema4C expression on migration ability of TLECs.** (A) TLECs
578 treated with lentivirus medium only (con), lentivirus vector control for Sema4C
579 siRNA (LV3NC), lentivirus vector control for full-length Sema4C (LV5NC), Sema4C
580 siRNA (LV3-siRNA), and full-length Sema4C (LV5-Sema4C). (B) TLECs with LV3-
581 siRNA or LV5-Sema4C were generated and confirmed by Sema4C mRNA expression
582 as measured by real-time PCR. (C) The migration ability of cells (con,
583 LV3NC,LV5NC,LV3-siRNA,and LV5-Sema4C) were assessed using a Transwell
584 assay. (D) Quantification of the number of cells at the bottom of the Transwell
585 chamber.

586 **Fig. 3 Role of Sema4C expression on EndMT of TLECs.** (A) Assessment of
587 mRNA expression levels of Sema4C, E-cadherin, and ERK1/2 using quantitative PCR.
588 (B) Protein expression levels of Sema4C, E-cadherin, p-ERK1/2, and total ERK
589 (ERK1/2) using western blot analysis. (C) Quantification of protein expression levels
590 of Sema4C, E-cadherin, p-ERK1/2, and total ERK (ERK1/2) using western blot. (D)
591 Intensity for p-ERK1/2 was normalized to total ERK1/2 and represent as fold change
592 over control group.

593 **Fig. 4 The ERK inhibitor can reverse migration ability of TLECs induced by**
594 **Sema4C.** (A) The migration ability in TLECs was assessed using only the media of
595 lentivirus (con), Sema4C siRNA (LV3-siRNA), full-length Sema4C (LV5-Sema4C),
596 LV3-siRNA cultured with PD98059, and LV5-Sema4C cultured with PD98059. (B)
597 Quantification of the number of cells from the bottom of the Transwell inserts was
598 measured.

599 **Fig. 5 Sema4C stimulates EndMT of TLECs via the ERK pathway.** (A-C) The
600 RNA expression levels of Sema4C, E-cadherin, and total ERK (ERK1/2) in TLECs
601 treated with only media of lentivirus (con), Sema4C siRNA (LV3-siRNA), full-length
602 Sema4C (LV5-Sema4C), LV3-siRNA cultured with PD98059, and LV5-Sema4C
603 cultured with PD98059. (D) The protein expression levels of Sema4C, E-cadherin, p-
604 ERK1/2, and total ERK (ERK1/2) in TLECs treated with only media of lentivirus
605 (con), Sema4C siRNA (LV3-siRNA), full-length Sema4C (LV5-Sema4C), LV3-
606 siRNA cultured with PD98059, and LV5-Sema4C cultured with PD98059 using
607 western blot analysis. (E-H) Quantification of protein expression levels of Sema4C,
608 E-cadherin, p-ERK1/2, and total ERK (ERK1/2). (I) Intensity for p-ERK1/2 was
609 normalized to total ERK1/2 and represent as fold change over control group. ns, no
610 significant difference.

Figures

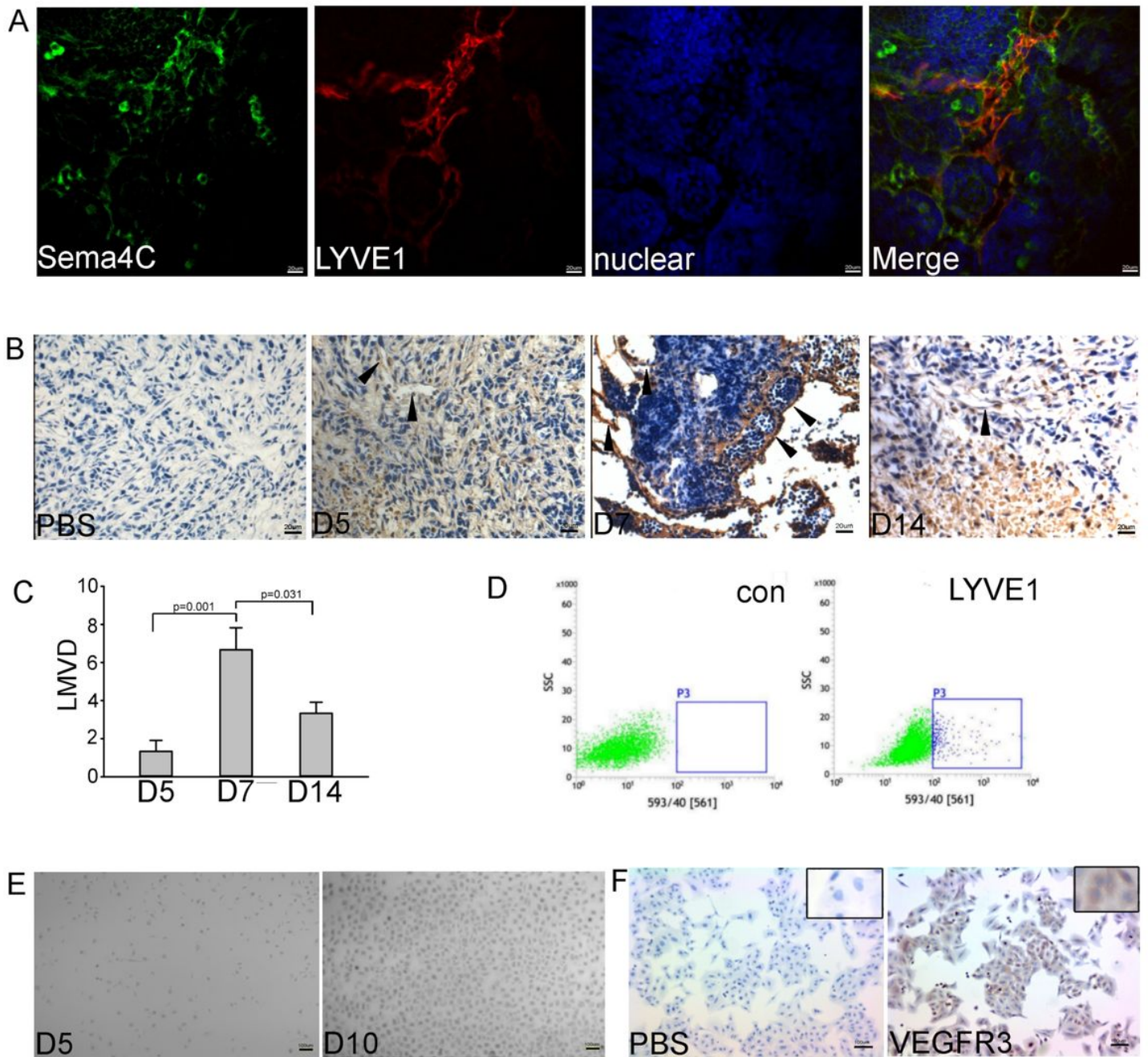


Figure 1

Tumor-associated lymphatic endothelial cells (TLECs) were obtained from a mouse xenograft tumor. (A) The location of Sema4C was detected in mouse tumor tissue. In lymphatic vessels, Sema4C (green) have co-location with LYVE1 (Red), one of the most notable marker for lymphatic endothelial cells. Nuclei were shown by DAPI staining (blue). (B) The most suitable time (the 7th day after U14 cells injection) for separation of TLECs was determined by LYVE1 immunohistochemical analysis. (C) Quantification of the

numbers of lymphatic vessels (LMVD) in 5th ,7th, 14th days were measured. (D) Tumor tissues were dissociated into a cell suspension and then stained for LYVE1-PE. LYVE1-positive cells were separated by flow cytometry. (E) TLECs were cultured in EBM-2 medium for 5 days and 10 days. (F) VEGFR3- positive TLECs were identified by immunohistochemistry.

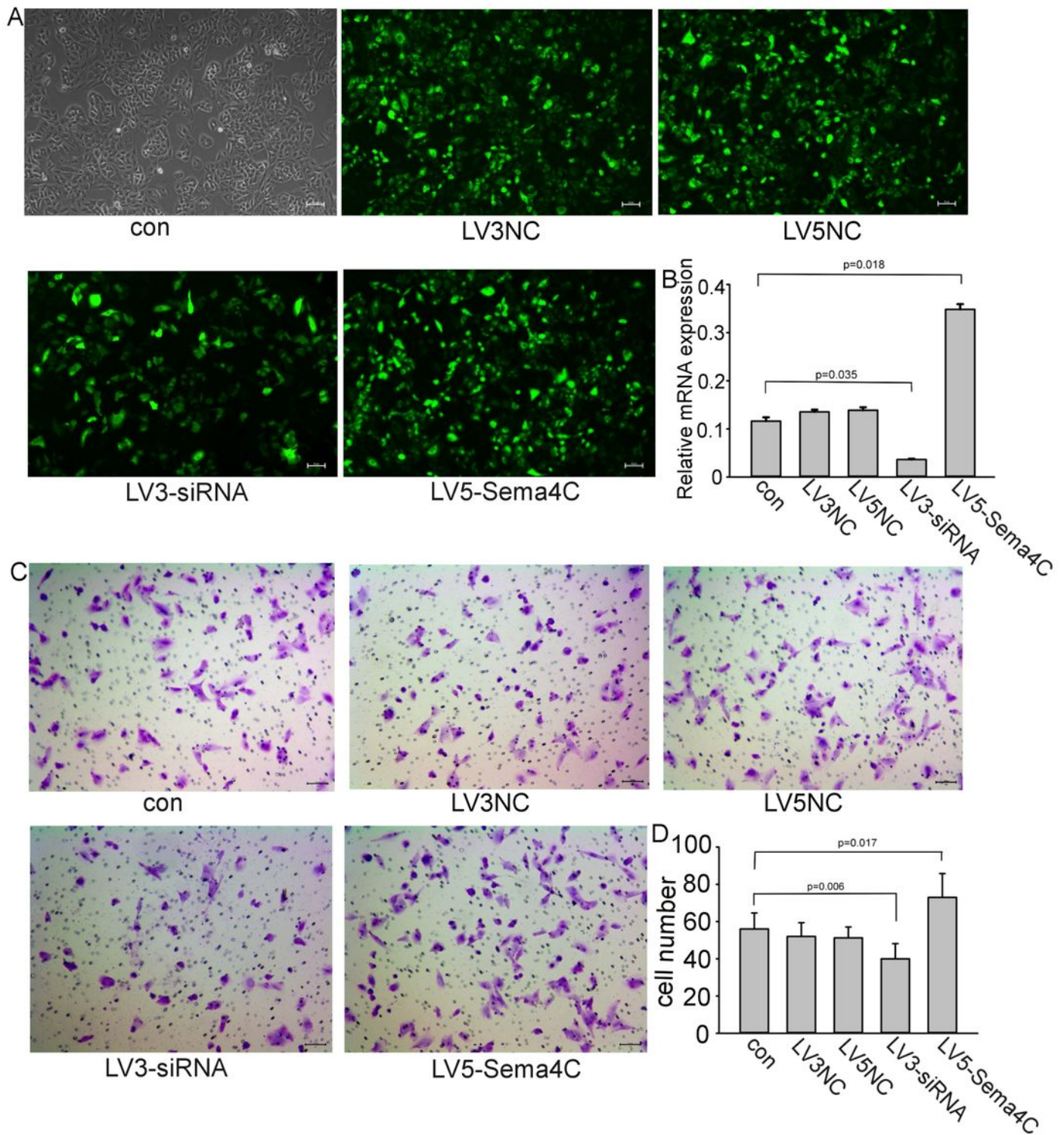


Figure 2

Role of Sema4C expression on migration ability of TLECs. (A) TLECs treated with lentivirus medium only (con), lentivirus vector control for Sema4C siRNA (LV3NC), lentivirus vector control for full-length Sema4C (LV5NC), Sema4C siRNA (LV3-siRNA), and full-length Sema4C (LV5-Sema4C). (B) TLECs with LV3- siRNA or LV5-Sema4C were generated and confirmed by Sema4C mRNA expression as measured by real-time PCR. (C) The migration ability of cells (con, LV3NC, LV5NC, LV3-siRNA, and LV5-Sema4C) were assessed using a Transwell assay. (D) Quantification of the number of cells at the bottom of the Transwell chamber.

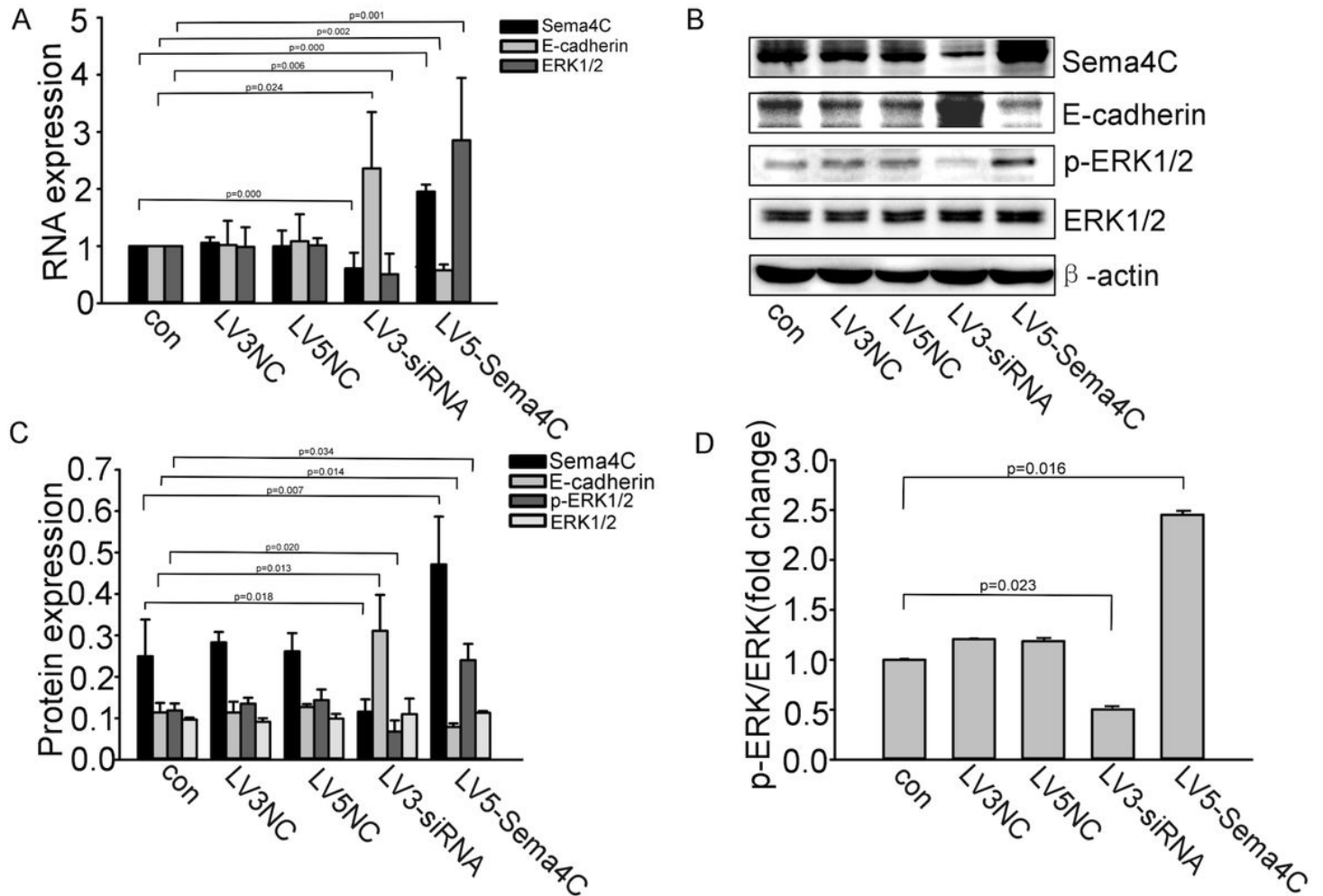


Figure 3

Role of Sema4C expression on EndMT of TLECs. (A) Assessment of mRNA expression levels of Sema4C, E-cadherin, and ERK1/2 using quantitative PCR. (B) Protein expression levels of Sema4C, E-cadherin, p-ERK1/2, and total ERK (ERK1/2) using western blot analysis. (C) Quantification of protein expression levels of Sema4C, E-cadherin, p-ERK1/2, and total ERK (ERK1/2) using western blot. (D) Intensity for p-ERK1/2 was normalized to total ERK1/2 and represent as fold change over control group.

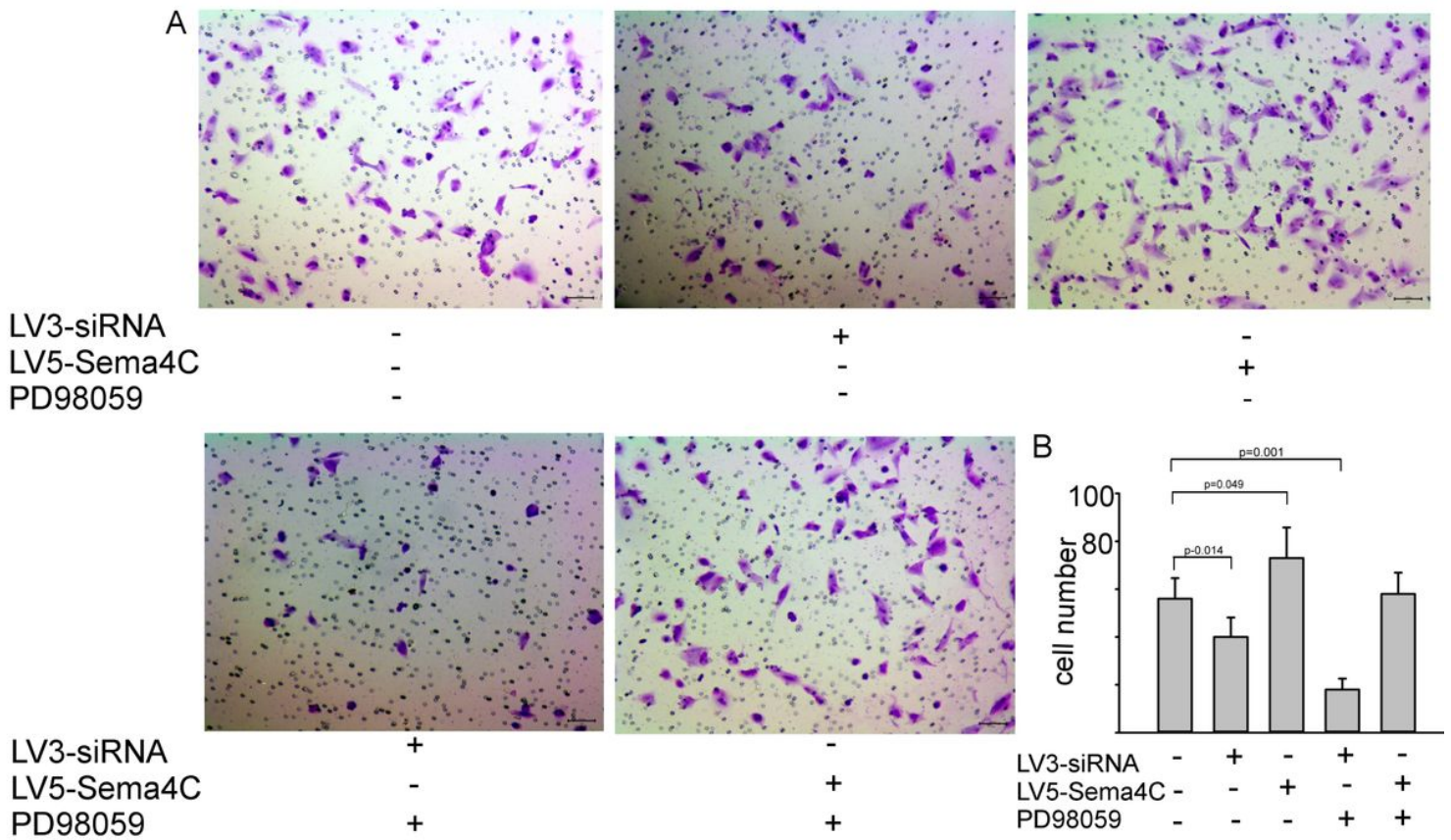


Figure 4

The ERK inhibitor can reverse migration ability of TLECs induced by Sema4C. (A) The migration ability in TLECs was assessed using only the media of lentivirus (con), Sema4C siRNA (LV3-siRNA), full-length Sema4C (LV5-Sema4C), LV3-siRNA cultured with PD98059, and LV5-Sema4C cultured with PD98059. (B) Quantification of the number of cells from the bottom of the Transwell inserts was measured.

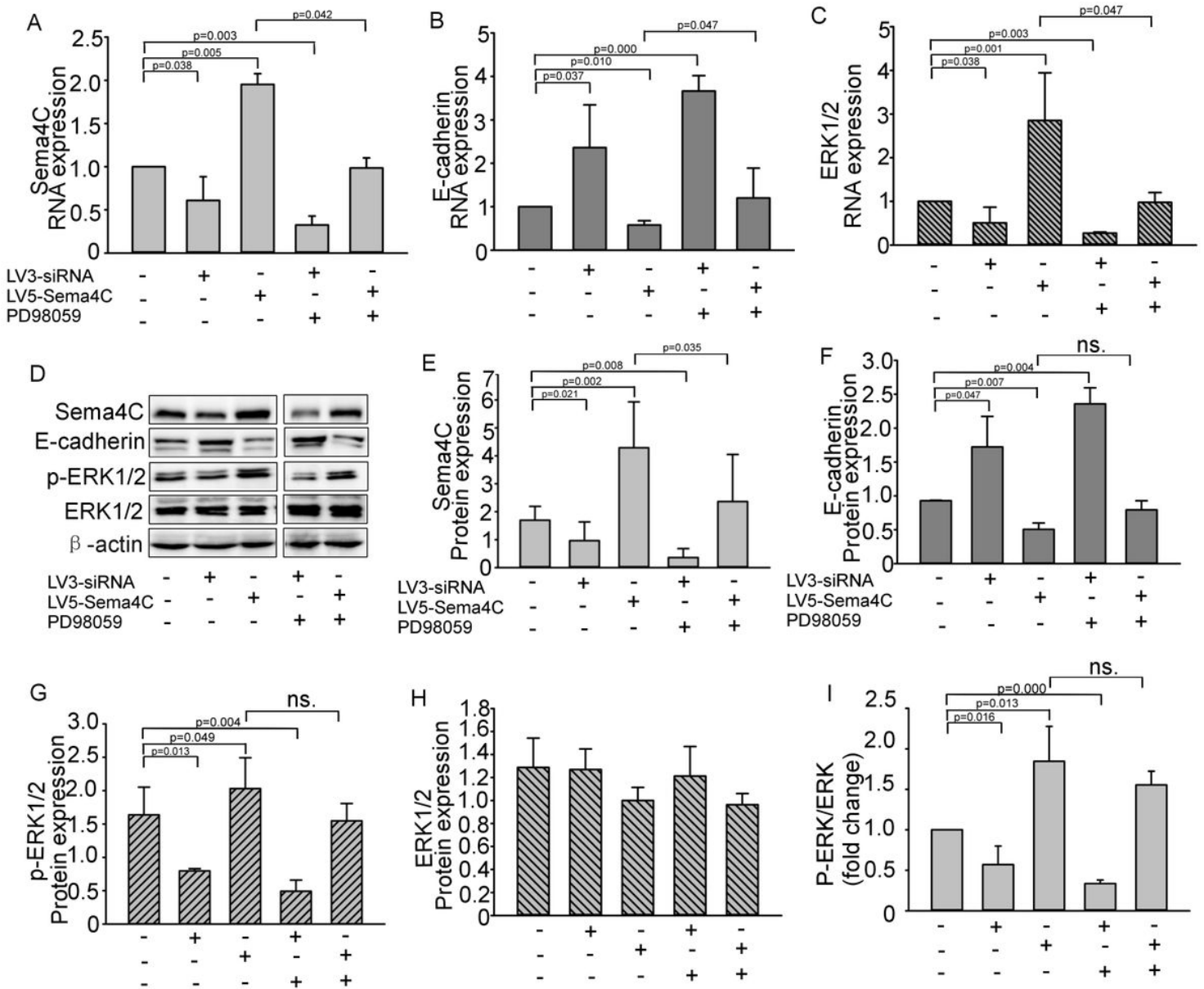


Figure 5

Sema4C stimulates EndMT of TLECs via the ERK pathway. (A-C) The RNA expression levels of Sema4C, E-cadherin, and total ERK (ERK1/2) in TLECs treated with only media of lentivirus (con), Sema4C siRNA (LV3-siRNA), full-length Sema4C (LV5-Sema4C), LV3-siRNA cultured with PD98059, and LV5-Sema4C cultured with PD98059. (D) The protein expression levels of Sema4C, E-cadherin, p-ERK1/2, and total ERK (ERK1/2) in TLECs treated with only media of lentivirus (con), Sema4C siRNA (LV3-siRNA), full-length Sema4C (LV5-Sema4C), LV3-siRNA cultured with PD98059, and LV5-Sema4C cultured with PD98059 using western blot analysis. (E-H) Quantification of protein expression levels of Sema4C, E-cadherin, p-ERK1/2, and total ERK (ERK1/2). (I) Intensity for p-ERK1/2 was normalized to total ERK1/2 and represent as fold change over control group. ns, no significant difference.